International Journal of Minerals, Metallurgy and Materials
Volume 17, Number 1, February 2010, Page 86
DOI: 10.1007/s12613-010-0115-0

Effect of SiO_2 addition on the microstructure and electrical properties of ZnO-based varistors

Zhen-hong Wu[1)], *Jian-hui Fang*[1,2)], *Dong Xu*[3)], *Qin-dong Zhong*[3)], *and Li-yi Shi*[1,3)]

1) Research Center of Nano Science and Technology, Shanghai University, Shanghai 200444, China

2) School of Science, Shanghai University, Shanghai 200444, China

3) School of Material Science and Engineering, Shanghai University, Shanghai 200072, China

(Received: 5 January 2009; revised: 10 February 2009; accepted: 17 February 2009)

Abstract: The microstructure and electrical properties of ZnO-based varistors with the SiO_2 content in the range of 0-1.00mol% were prepared by a solid reaction route. The varistors were characterized by scanning electron microscopy, X-ray diffraction, energy-dispersive X-ray spectrometry, inductively coupled plasma-atomic emission spectrometry, and X-ray photoelectron spectroscopy. The results indicate that the average grain size of ZnO decreases with the SiO_2 content increasing. A new second phase (Zn_2SiO_4) and a glass phase (Bi_2SiO_5) are found. Element Si mainly exists in the grain boundary and plays an important role in controlling the Bi_2O_3 vaporization. The electric measurement shows that the incorporation of SiO_2 can significantly improve the nonlinear properties of ZnO-based varistors, and the nonlinear coefficients of the varistors with SiO_2 are in the range of 36.8-69.5. The varistor voltage reaches the maximum value of 463 V/mm and the leakage current reaches the minimum value of 0.11 μA at the SiO_2 content of 0.75mol%.

Keywords: inorganic materials; varistor; silicon dioxide; electrical properties

1. Introduction

ZnO-based varistors are polycrystalline ceramic devices which exhibit highly nonlinear current-voltage characteristics that are often expressed by $I=KV^{\alpha}$, where K is a constant, V is the voltage, and α is the nonlinear exponent [1-2]. This extensive nonohmic characteristic together with an ability of repeatedly withstanding relatively high power pulses has resulted in the widespread application of varistors as voltage surge protectors in electrical circuits since the 1970s [3-4]. Most commonly varistors are produced by sintering ZnO powder together with small amounts of oxide additives, such as Sb_2O_3, Bi_2O_3, Co_2O_3, MnO_2, and Cr_2O_3 [5-9]. These oxide additions can affect the varistor properties in two ways: (1) directly, in an electrical sense, as in the case of Bi_2O_3 which segregates at the grain boundaries and relates to the nonlinearity of the current voltage characteristics [6, 10]; (2) indirectly, by affecting the microstructural development of a ceramic body during firing. One interesting group of additive oxides is that which reacts with ZnO to form a second phase with the spinel structure, such as Sb_2O_3 and Al_2O_3 [5, 11]. The other is Bi_2O_3, as a sintering aid due to the formation of a ZnO-Bi_2O_3 eutectic at 750ºC, plays an essential role in imparting nonlinear behavior to the material [12]. However, the Bi_2O_3 liquid phase starts to vaporize from its inception and keeps vaporizing during the entire sintering procedure. This means that the composition is likely to change after sintering due to the Bi_2O_3 vaporization which may affects the properties of ZnO varistors [7, 13].

Recently, several literatures [14-16] reported that SiO_2 could control the sintering mechanism, tremendously enhance the nonlinearity, and increase the density of traps considerably. In the present study, ZnO-Bi_2O_3 varistors were fabricated with the SiO_2 additive to scrutinize the effect of SiO_2 content on the microstructure, and hence the electrical properties of ZnO-Bi_2O_3 varistors, such as the breakdown voltage, leakage current, nonlinear coefficient, and field current density (E-J) characteristics, could be improved significantly. In addition, the Bi_2O_3 vaporization affected by

Corresponding author: Li-yi Shi E-mail: sly0726@163.com

the SiO_2 content was also discussed.

2. Experimental procedure

2.1. Sample preparation

ZnO-based varistor samples with the composition of (96.50–*x*)mol% ZnO+0.70mol% Bi_2O_3+1.00mol% Sb_2O_3+0.80mol% Co_2O_3+0.50mol% Cr_2O_3+0.50mol% MnO_2+*x*mol% SiO_2 for *x*=0, 0.25, 0.50, 0.75, and 1.00 (samples labeled a, b, c, d, and e, respectively) were chosen for investigation. The reagent-grade ZnO powder and additives were milled together in ethanol in a polyethylene jar for 5 h using zirconia balls as the milling media in a planetary ball mill operated at 500 r/min. The mixture was dried at 70ºC for 24 h. After 2wt% polyvinyl alcohol binder addition, the mixture was milled again using an agate mortar to produce the starting powder. The powder was uniaxially pressed into disks of 12 mm in diameter and 2 mm in thickness, and around 56% of the theoretical density (TD, 5.67 g/cm^3). The green pellets were placed on an alumina crucible covered with ZnO powders to separate the samples from the alumina crucible and prevent material diffusion into the substrate, then were sintered in air at 1100ºC for 2 h at a heating rate of 5ºC/min followed by cooling in the furnace.

2.2. Microstructure analysis

For microstructure analysis, the cross-section of the samples were ground and polished, then part of the samples were etched chemically by dilute acid for about 10 min to expose the grain boundaries for the stereological analysis. The surface microstructures were examined by a scanning electron microscope (SEM, FEI QUANTA 400) in a back-scattered electron (BE) mold. The other polished (un-etched) part of the samples were used to analyze the phase composition by X-ray diffractometry (XRD, Rigaku D/max 2200, Japan) using a Cu K_α radiation. The compositional analysis of the selected areas was determined in the SEM by energy dispersive X-ray spectrometry (EDS). The X-ray photoelectron spectrum (XPS) was recorded on a PHI-5000C ESCA system (Perkin Elmer) with Al K_α radiation. The average grain sizes (*d*) were determined by the linear intercept method, given by $d=1.56L/MN$, where *L* is the random line length on the micrograph, *M* is the magnification of the micrograph, and *N* is the number of the grain boundaries intercepted by lines [17]. The Bi_2O_3 content of the sintered varistors was measured using an inductively coupled plasma-atomic emission spectrometer (ICP-AES) (Perkin-Elmer, America). The density of the pellets (ρ) was measured geometrically.

2.3. Electrical measurements

To measure the electrical properties, silver paste was placed on both surfaces of the samples and heated at 600ºC for 10 min. The size of electrodes was 5 mm in diameter. The electric field strength-current density (*E*-*J*) characteristics were measured using a DC parameter instrument for varistor (Model CJ1001). The nominal varistor voltages (V_N) at 0.1 mA ($V_{0.1\ mA}$) and 1 mA ($V_{1\ mA}$) were measured. The threshold voltage (V_T, V/mm), which was the breakdown voltage per unit thickness of varistor ceramic, was measured by $V_T=V_{1\ mA}/d$, where *d* was the thickness of the sample in mm. The leakage current (I_L) was measured at $0.75V_{1\ mA}$. The nonlinear coefficient (α) was obtained from the equation $\alpha=1/\lg(V_{1\ mA}/V_{0.1\ mA})$ [2].

3. Results and discussion

3.1. Microstructure

Fig. 1(a) shows the XRD patterns of the samples with different SiO_2 contents. The patterns show the existence of $Zn_7Sb_2O_{12}$ spinel phase and the Bi-rich phase in all the samples in addition to the ZnO phase. The additional peak of Zn_2SiO_4 phase is only found in the sample with the SiO_2 content of 1.00mol%, while other samples do not show the additional peak because of their small amount of SiO_2, *i.e.*, less than 1.00mol%. In addition, a new phase, Bi_2SiO_5, is found in all the samples, the peaks of which are very weak at 29.28°, shown as the local magnified image in Fig. 1(b). Bi_2SiO_5, as a glass phase, can make the liquid phase wet the grain boundaries more easily, and is helpful to the atomic Bi absorbed on the surfaces of ZnO grains. Thus, the addition of SiO_2 is helpful in controlling the Bi_2O_3 vaporization from ZnO-based varistors.

Fig. 2 shows the back-scattered electron images (BEI) of the samples with different SiO_2 contents. The microstructures do not have much difference from each other with increasing the SiO_2 content except for the grain size. The sample with 0.50mol% SiO_2 appears more homogeneous in comparison to other samples. The average grain size of the samples determined by the linear intercept method is presented in Fig. 3. It markedly decreases with increasing the SiO_2 content, which can be accounted by the generation of the secondary phase (Zn_2SiO_4 and $Zn_7Sb_2O_{12}$). Beyond the SiO_2 content of 0.50mol%, the average grain size of ZnO changes a little. Fig. 3 also presents the density (ρ) of the samples with different SiO_2 contents. It increases first and then decreases. The sample with 0.50mol% SiO_2 exhibits the highest density at 5.52 g/cm^3 corresponding to 97.69%

of the theoretical density (5.65 g/cm^3 in ZnO). In addition, doping Sb_2O_3 to the ZnO-Bi_2O_3 based varistors results in the formation of inversion boundaries (IBs), shown in Fig. 2(a). Recent findings [18-20] have revealed that IBs play a crucial role *via* the so-called IBs-induced grain-growth mechanism and microstructural development of varistor ceramics. It is generally known that IBs are related to the Sb_2O_3/Bi_2O_3 ratio, and the amount of Bi_2O_3 is affected by the sintering process.

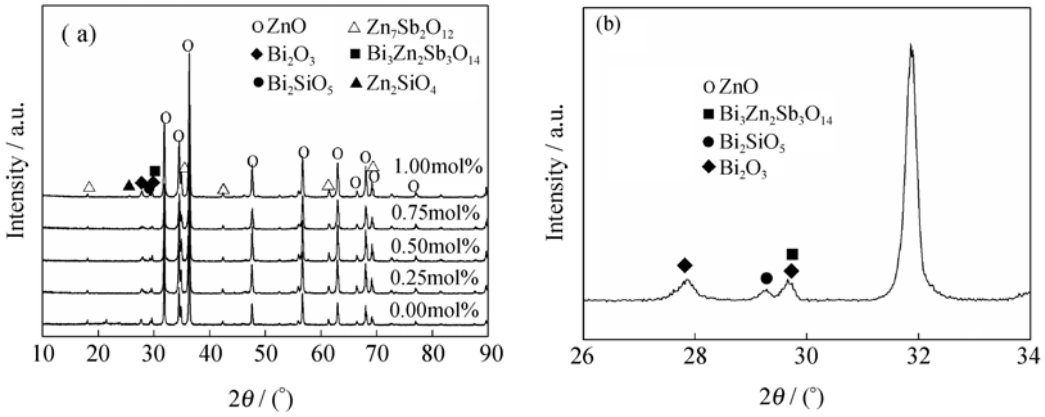

Fig. 1. XRD patterns of the samples: (a) with different SiO_2 contents; (b) with the SiO_2 content of 1.00mol%.

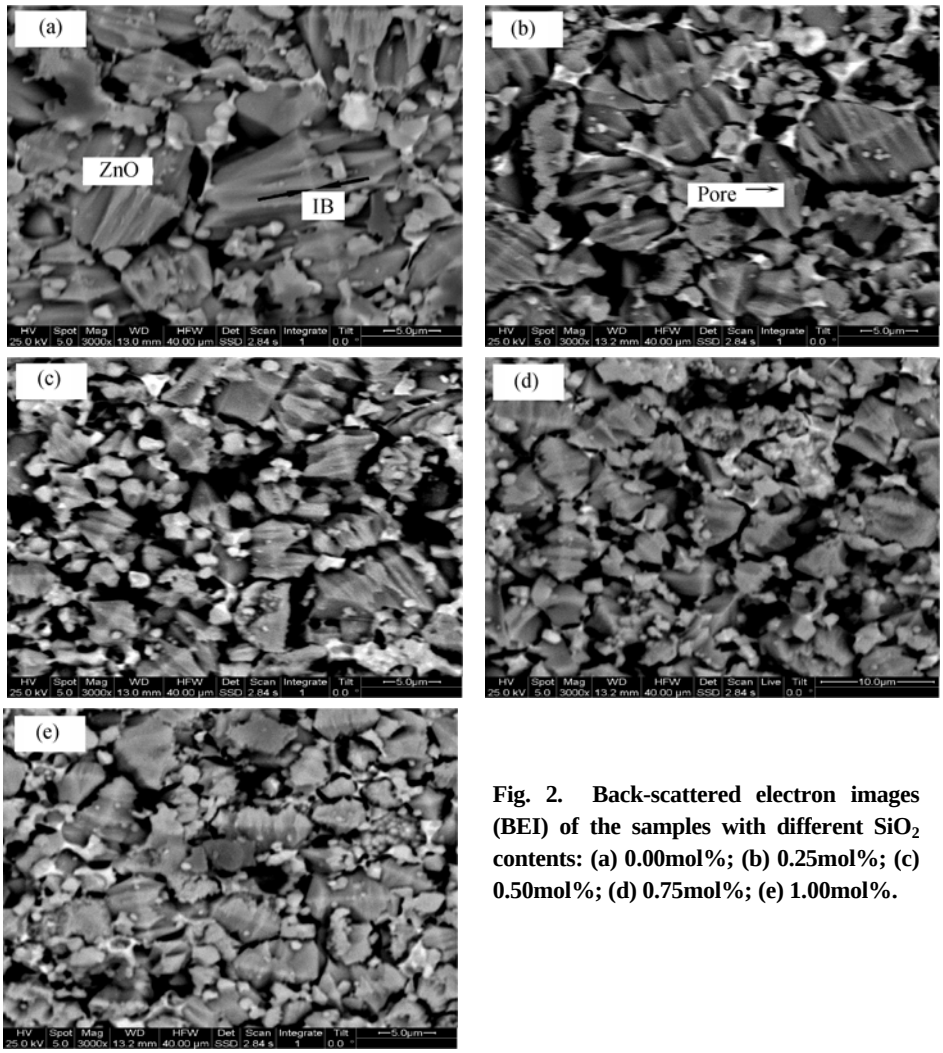

Fig. 2. Back-scattered electron images (BEI) of the samples with different SiO_2 contents: (a) 0.00mol%; (b) 0.25mol%; (c) 0.50mol%; (d) 0.75mol%; (e) 1.00mol%.

Fig. 4(A) shows the wide survey XPS spectra of samples (a) and (e), the composites mainly contain elements Zn, O,

and C (contamination carbon). Fig. 4(B) shows that the binding energy of the Si2p photoelectron peak is 103 eV, which is neither the peak of pure Si (99.5 eV) nor that of Si^{4+} in SiO_2 (103.6 eV) [21].

As shown in Fig. 4(D), the binding energy of the O1s photoelectron peak of sample (e) is 532.2 eV (the standard value is 532.5 eV), it shifts to high binding energies compared to sample (a). These results indicate that element O is a little deficient in the SiO_2 crystal lattice and SiO_2 is the main existence form of Si and O elements in sample (e). Fig. 4(C) displays the binding energies of Zn2p for samples (a) and (e). The binding energy for Zn2p of sample (a) is 1020.1 eV. After doping 1.00mol% SiO_2, the peak shifts to the higher binding energy of 1022.4 eV. This can be explained as element Si is substitutional or interstitial at the Zn site of the ZnO crystal, and then a chemical-defect reaction is created. Using Kroger-Vink notation, the reaction can be expressed as

$$2SiO_2 \rightarrow Si_{Zn}^{2+} + 2e + SiO_2 + O_2,$$

where Si_{Zn}^{2+} is two positively charged Si ions substituted for Zn lattice site.

SiO_2, as glass phase, has high insulation. The oxygen generated in the above reaction affects the donor concentration. Si_{Zn}^{2+} as a positive charged center can enhance the ability of bound electron, and then make the binding energy of Zn2p shift higher. This was further confirmed by the EDS study (Fig. 5) which obviously showed the presence of Si peaks at the grain boundary as well as within the grain.

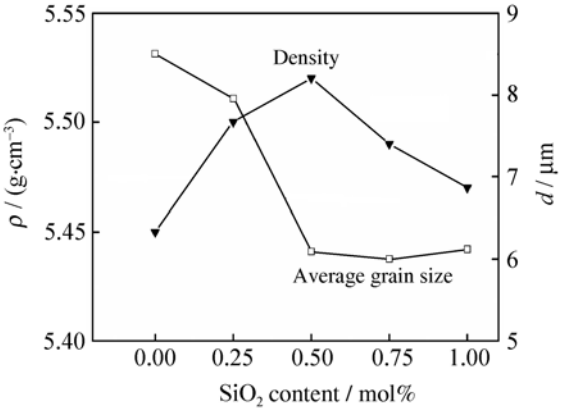

Fig. 3. Density (ρ) and average grain size (d) of the samples with different SiO_2 contents.

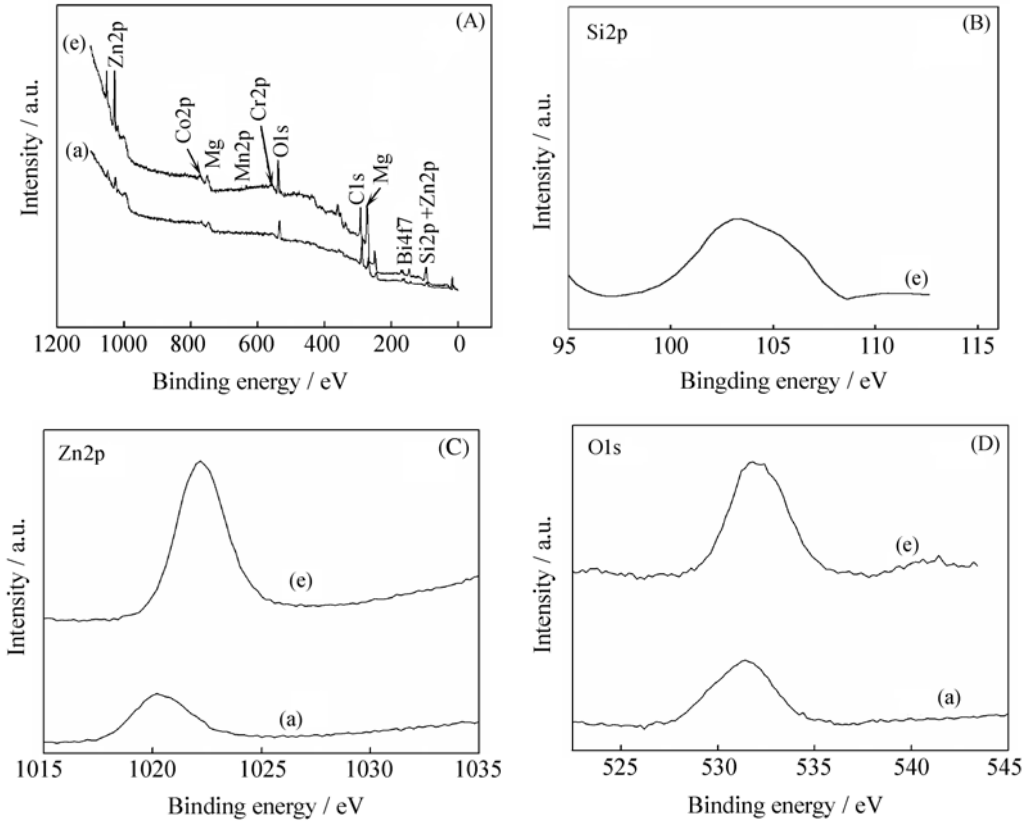

Fig. 4. Wide survey XPS spectra of samples (a) and (e) (A), XPS Si2p spectra of sample (e) (B), XPS Zn2p spectra of samples (a) and (e) (C), and XPS O1s spectra of samples (a) and (e) (D).

3.2. Electrical characteristics

Table 1 shows the *V-I* characteristic parameters of the varistors. It can be seen that the nonlinear coefficient (α) of the varistor without SiO_2 is 29.5, whereas the value of α of the varistors with SiO_2 abruptly increases in the range of 36.8-69.5. The maximum value of α is obtained at 1.00mol% SiO_2. Furthermore, it is changed a little beyond the SiO_2 content of 0.75mol%. The leakage currents are all less than 0.5 μA, and the minimum value is 0.11 μA at 0.75mol% SiO_2. As the SiO_2 content increases, V_T first increases and then decreases. It reaches the maximum of 463 V/mm at the SiO_2 content of 0.75mol%. The results indicate that the varistor with 0.75mol% SiO_2 has the best electrical properties. The amount of Bi_2O_3 vaporization of the samples with SiO_2 are all lower than that without SiO_2, which can be attributed to the formation of Bi_2SiO_5 phase and Zn_2SiO_4 phase.

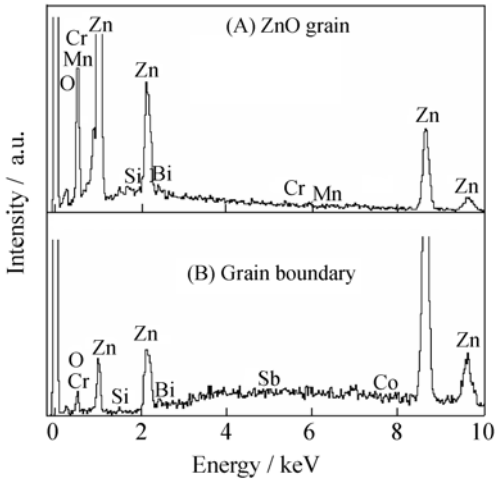

Fig. 5. EDS analysis of the samples with 0.75mol% SiO_2.

Table 1. *V-I* characteristic parameters and Bi_2O_3 vaporization of the samples with different SiO_2 contents

SiO_2 content / mol%	V_T / (V·mm^{-1})	I_L / μA	Bi_2O_3 vaporization / wt%	α
0.00	332	0.15	28.4	29.5
0.25	355	0.38	15.9	36.8
0.50	462	0.16	18.0	48.3
0.75	463	0.11	21.6	67.7
1.00	460	0.12	19.5	69.5

Fig. 6 shows the electric field strength-current density (*E-J*) characteristics of ZnO-based varistors with different SiO_2 contents. It shows that all the samples have similar *E-J* curves with a sharp transition from the low current zones to the nonlinear regions. The electrical conduction characteristics are divided into two regions: a linear *E-J* relationship before the critical operation field and a nonlinear *E-J* relationship after the critical operation field. Nahm [22] reported that the sharper the knee of the curves between the two regions was, the better the nonlinear properties were. In Fig. 6, only samples (a) and (b) show a much gentler transition indicating a poor electrical response. This result is consistent with the characteristic parameters shown in Table 1.

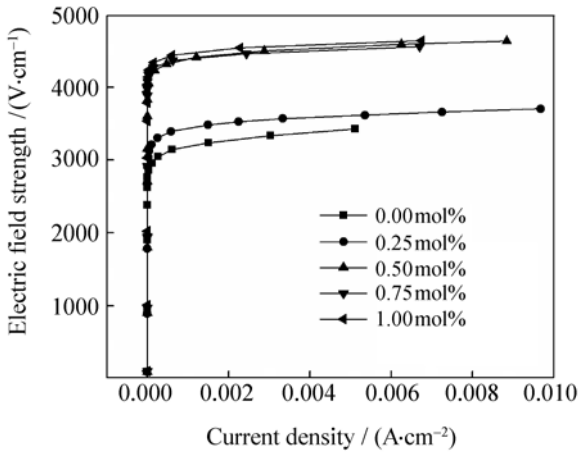

Fig. 6. *E-J* characteristics of the samples with various SiO_2 contents

4. Conclusions

ZnO-based varistors were prepared with different SiO_2 contents by a solid reaction route. The average grain size of ZnO decreases from 8.50 to 5.85 μm with the SiO_2 content increasing. The analyses using EDS and XPS indicate that element Si distributes in the grain boundary as well as in the grains. Two new phases, Zn_2SiO_4 and Bi_2SiO_5, are found in the varistors with SiO_2. The results of ICP-AES show that the amount of Bi_2O_3 vaporization in all the varistors with SiO_2 is lower than that without SiO_2. V_T and α of the varistors increase with the SiO_2 content increasing. V_T reaches the maximum value of 463 V/mm at the SiO_2 content of 0.75mol%, and α reaches the maximum value of 69.5 at the SiO_2 content of 1.00mol%, respectively. The I_L exhibits a minimum value of 0.11 μA at 0.75mol% SiO_2. Considering all the data of electrical properties and density, the best value of SiO_2 addition in ZnO-based varistors is 0.75mol%.

References

[1] D.R. Clarke, Varistor ceramics, *J. Am. Ceram. Soc.*, 82(1999), p.485.

[2] D. Xu, L. Shi, Z. Wu, *et al.*, Microstructure and electrical

properties of ZnO-Bi_2O_3-based varistor ceramics by different sintering processes, *J. Eur. Ceram. Soc.*, 29(2009), p.1789.

[3] M. Matsuoka, Nonohmic properties of zinc oxide ceramics, *Jpn. J. Appl. Phys.*, 10(1971), p.736.

[4] T.K. Gupta, Applications of zinc oxide ceramics, *J. Am. Ceram. Soc.*, 73(1990), p.1817.

[5] T. Takemura, M. Kobayashi, Y. Takada, and K. Sato, Effects of antimony oxide on the characteristics of ZnO varistors, *J. Am. Ceram. Soc.*, 70(1987), p.237.

[6] E. Olsson and G.L. Dunlop, The effect of Bi_2O_3 content on the microstructure and electrical properties of ZnO varistor materials, *J. Appl. Phys.*, 66(1989), p.4317.

[7] M. Peiteado, M.A. De, M.J. Velasco, *et al.*, Bi_2O_3 vaporization from ZnO-based varistors, *J. Eur. Ceram. Soc.*, 25(2005), p.675.

[8] C.C. Lin, W.S. Lee, C.C. Sun, and W.H. Whu, The influences of bismuth antimony additives and cobalt manganese dopants on the electrical properties of ZnO-based varistors, *Compos. Part B*, 38(2007), p.338.

[9] S.G. Cho, H. Lee, and H.S. Kim, Effect of chromium on the phase evolution and microstructure of ZnO doped with bismuth and antimony, *J. Mater. Sci.*, 32(1997), p.4283.

[10] K.O. Magnusson and S. Wiklund, Interface formation of Bi on ceramic ZnO: a simple model varistor grain boundary, *J. Appl. Phys.*, 76(1994), p.7405.

[11] S. Bernik and N. Daneu, Characteristics of ZnO-based varistor ceramics doped with Al_2O_3, *J. Eur. Ceram. Soc.*, 27(2007), p.3161.

[12] J. Ott, A. Lorenz, M. Harrer, *et al.*, The influence of Bi_2O_3 and Sb_2O_3 on the electrical properties of ZnO-based varistors, *J. Electroceram.*, 6(2001), p.135.

[13] C. Lin, Z. Xu, P. Hu, and D.F. Sun, Bi_2O_3 vaporization in microwave-sintered ZnO varistors, *J. Am. Ceram. Soc.*, 90(2007), p.2791.

[14] R. Einzinger, Metal oxide varistors, *Ann. Rev. Mater. Sci.*, 17(1987), p.299.

[15] T.R.N. Kutty and S. Ezhilvalavan, The role of silica in enhancing the nonlinearity coefficients by modifying the trap states of zinc oxide ceramic varistors, *J. Phys. D*, 29(1996), p.809.

[16] S.J. So and C.B. Park, Improvement in the electrical stability of semiconducting ZnO ceramic varistors with SiO_2 additive, *J. Korean Phys. Soc.*, 40(2002), p.925.

[17] C.W. Nahm, Effect of cooling rate on degradation characteristics of $ZnO{\cdot}Pr_6O_{11}{\cdot}CoO{\cdot}Cr_2O_3{\cdot}Y_2O_3$-based varistors, *Solid State Commun.*, 132(2004), p.213.

[18] B.A. Haskell, S.J. Souri, and M.A. Helfand, Varistor behavior at twin boundaries in ZnO, *J. Am. Ceram. Soc.*, 82(1999), p.2106.

[19] A. Rečnik, N. Daneu, T. Walther, and W. Mader, Structure and chemistry of basal-plane inversion boundaries in antimony oxide doped zinc oxide, *J. Am. Ceram. Soc.*, 84(2001), p.2657.

[20] S. Bernik, N. Daneu, and A. Rečnik, Inversion boundary induced grain growth in TiO_2 or Sb_2O_3 doped ZnO-based varistor ceramics, *J. Eur. Ceram. Soc.*, 24(2004), p.3703.

[21] C.N. Ye, N.Y. Tang, X.M. Wu, *et al.*, XPS analysis of Ge-SiO_2 thin film, *Microfabr. Technol.* (in Chinese), 1(2002), p.36.

[22] C.W. Nahm, The effect of sintering temperature on electrical properties and accelerated aging behavior of PCCL-doped ZnO varistors, *Mater. Sci. Eng. B*, 136(2007), p.134.